ISBN: 978-3-95450-132-8 doi:10.18429/JACoW-IPAC2014-THPRO042

FIELD EMISSION STUDIES OF HEAT TREATED MO SUBSTRATES

R. Barday*, A. Jankowiak, T. Kamps, C. Klimm, J. Knobloch, F. Siewert, A. Varykhalov,
Helmholtz-Zentrum Berlin für Materialien und Energie GmbH, Germany
B. Senkovskiy, Institut für Festkörperphysik, TU Dresden, Germany
S. Lagotzky, G. Müller, FB C Physics Department, University of Wuppertal, Germany

Abstract

Molybdenum can be used as a substrate for bi-alkali antimonide photocathodes utilized for the generation of high brightness electron beams in superconducting radio frequency (SRF) photoinjector cavities. Operation at high field strength is required to obtain a low emittance beam, thus increasing the probability of field emission (FE) from the cathode surface. Usually, substrates are heated *in situ* before alkali deposition to remove oxide layers from the surface. FE on Mo substrates was measured by means of a field emission scanning microscope (FESM). It turned out that *in situ* heat treatment (HT) of the Mo surface significantly changes the FE behaviour by activation of new emitters. For a better understanding of the mechanism for enhanced emission after *in situ* heating a witness Mo sample was investigated using x-ray photoelectron spectroscopy.

INTRODUCTION

The integration of a photocathode into the cavity with low contribution to the dark current is one of the major challenges for the development of SRF guns. It was demonstrated that CsK_2Sb cathodes with high quantum efficiency can be grown on Si substrates [1]. However, large dielectric losses of Si inhibit its implementation in the SRF guns. Instead, Mo can be used as a substrate. Typically, only the center of the substrate is coated with photocathode material to reduce a production of an unwanted beam for example through laser stray light. Hence substrate material is also exposed to the RF field, for this reason we also want to understand and prevent FE from Mo. In this paper we describe our studies of FE on Mo substrates and mechanisms leading to enhanced FE.

EXPERIMENTAL DETAILS

The Mo sample with a diameter of 10 mm and a rounded edge $r \sim 0.3$ mm was mechanically polished to an rms surface roughness in the flat part of about $S_q < 2$ nm and peak-to-valley of $S_t < 40$ nm as measured by a white-light interferometer (magnification 20x, 235 µm^2) and an rms $S_q < 1$ nm as measured by an atomic force microscope in non-contact mode on a view field of 25 µm^2. The sample was first cleaned with ionized nitrogen followed by dry ice cleaning under ISO class 2 cleanroom conditions. Then the sample was protected by a Teflon cap to avoid any damages or dust contaminations during the sample transport to the FESM [2]. After the sample was inserted into the load-lock chamber of the FESM, it was pumped down, the protection cap was removed at a pressure of about 10^{-7} mbar, and the sample was transferred into the analysing chamber with a base pressure of about 10^{-9} mbar. Samples can be annealed in the load-lock of the FESM up to 1200 °C.

FE measurements were performed over the entire surface including the rounded edges. During the scan the applied voltage is adjusted for a maximum of 1 nA emission current to avoid emitter modification through the current conditioning. The field strength for a constant gap d between the substrate and the anode tip is adjusted using a 10 kV power supply. The gap is maintained using a XYZ-stage, which consists of a stepper motor table and a piezo translator and is controlled by a long-distance optical microscope and a CCD video camera with an accuracy of about ±10 µm. In general, the electric field depends on the anode shape, tip radius and the gap. For the tungsten anode in the form of a truncated cone of 300 µm in diameter and a gap of 50 µm the field strength was estimated just as a ratio of the applied voltage to the gap. Guided by the FE maps, local $I(E)$ measurements were carried out to characterize the emitters in terms of the enhancement factor β and the onset field E_{on}, which is defined as a field required for 1 nA emission current. The resulting curves are fitted by the modified Fowler-Nordheim (FN) equation [3]:

$$I = A_e a (\beta E)^2 \phi^{-1} t_N^{-2} \exp\left(-b\phi^{1.5} \nu_N (\beta E)^{-1}\right), \quad (1)$$

where I is the emission current (A), A_e is the effective area of the emitter (m^2), E is the macroscopic electric field (V/m), ϕ is the work function (eV), $a = 1.54 \cdot 10^{-6}$ A eV V^{-2} and $b = 6.83 \cdot 10^9$ eV$^{-1.5}$ V m^{-1} are universal constants, t_N and ν_N are tabulated dimensionless elliptic functions, which were set to 1. For the local measurements the gap is controlled with higher accuracy than for the field map measurements. For this purpose the anode tip is centered at the emission site, then the voltage required to keep the current constant as a function of the gap is measured. An extrapolation of the $V(z)$ to the zero crossing yields an accurate measure of the gap.

For a better understanding of the processes at the surface and the role of the oxides a polycrystalline witness Mo sample with a purity of 99.9 % was investigated using x-ray photoelectron spectroscopy (XPS) at the Russian-German beamline of the synchrotron radiation source BESSY II [4]. The XPS spectrum of the Mo 3d level, which is sensitive to the oxide contaminations, was measured at an incident photon energy of 650 eV. The base pressure in the analysing chamber during the measurement was about $4 \cdot 10^{-10}$ mbar.

* roman.barday@helmholtz-berlin.de

Content from this work may be used under the terms of the CC BY 3.0 licence (© 2014). Any distribution of this work must maintain attribution to the author(s), title of the work, publisher, and DOI.

ISBN: 978-3-95450-132-8 doi:10.18429/JACoW-IPAC2014-THPRO042

Content from this work may be used under the terms of the CC BY 3.0 licence (© 2014). Any distribution of this work must maintain attribution to the author(s), title of the work, publisher, and DOI.

RESULTS AND DISCUSSIONS

A first FE map of the unnealed Mo sample was performed at 180 MV/m about 1 week after the polishing. The major part of the emitters was located near the rounded edges of the sample and not on the flat surface, indicating a worse surface quality of the edge. Nevertheless the lowest onset field of 50 MV/m beyond the fields needed for SRF cavities. Then the sample was heated at 100 °C for 1 h. After the sample naturally cooled down in the load-lock chamber, it was transferred into the FESM chamber for further FE measurements. Additional cycles were carried out at 200 °C, 300 °C, 400 °C and 600 °C in the same sequence.

Up to the HT at 300 °C distribution of emitters has barely changed. The most dominant effect with many more emitters both at the edge and in the flat region was observed after HT at 400 °C, the number of the emitters has roughly doubled (Fig. 1). The distribution of the emitters after the last HT at 600 °C has slightly changed in comparison to HT at 400 °C, already activated emitters become stronger.

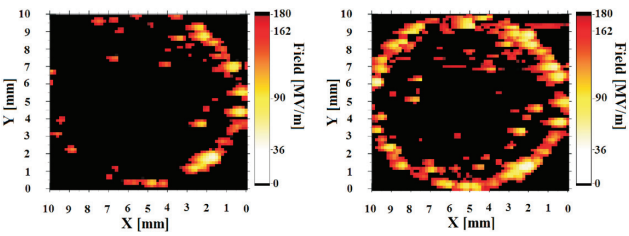

Figure 1: FE map of the single crystal Mo sample at maximum 180 MV/m after HT at 300 °C (left) and 400 °C (right).

In order to reduce FE, the sample was repolished and particular attention was paid to the edge. About two months after the repolishing a field map was taken again at E = 50 MV/m, which is a reasonable peak surface field for SRF cavity operation. No FE (<1 nA) was observed for the unnealed sample and after HT up to 400 °C. First emission was observed after HT at 500 °C at E_{on} ~20 MV/m, which is relevant for the applications in SRF guns (Fig. 2). The distribution of the emitters after HT at 600 °C hardly changed.

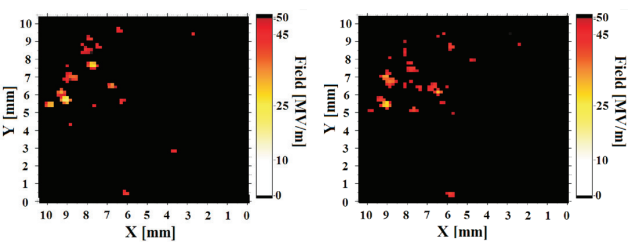

Figure 2: FE map of the single crystal Mo sample at maximum 50 MV/m after HT at 500 °C (left) and 600 °C (right).

Prior to HT the strongest emitters yielded E_{on} = 60 – 135 MV/m and β = 35 – 125. The range of these values became narrower after the final HT at 600 °C with E_{on} = 30 – 80 MV/m and β = 25 – 90. A typical example of the locally measured curves is shown in figure 3.

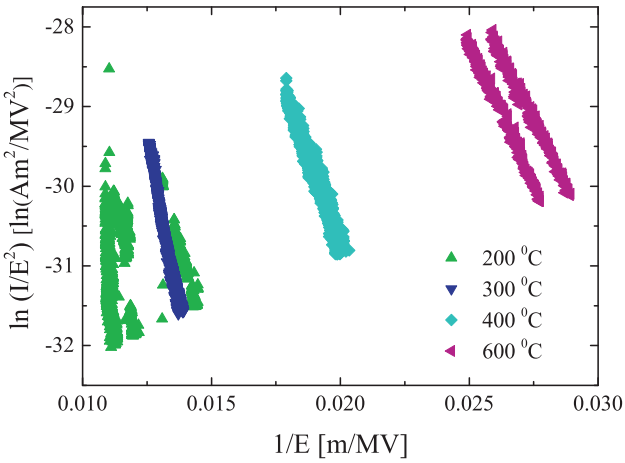

Figure 3: Example of FN plots for an emitter after HT at different temperatures.

Despite of slightly different behaviour of the various emitters after HT the following conclusions can be drawn:

- Emission becomes more stable
- Onset field E_{on} slightly shifted to lower values.

Most of the local emitters were finally investigated by means of scanning electron microscopy (SEM) and energy-dispersive x-ray spectroscopy (EDX). The images of two emitters are shown in figure 4. The EDX analysis of one emitter reveals tungsten contaminations; its origin is not completely understood, but it can not be excluded that some material transfer from the anode to the cathode took place.

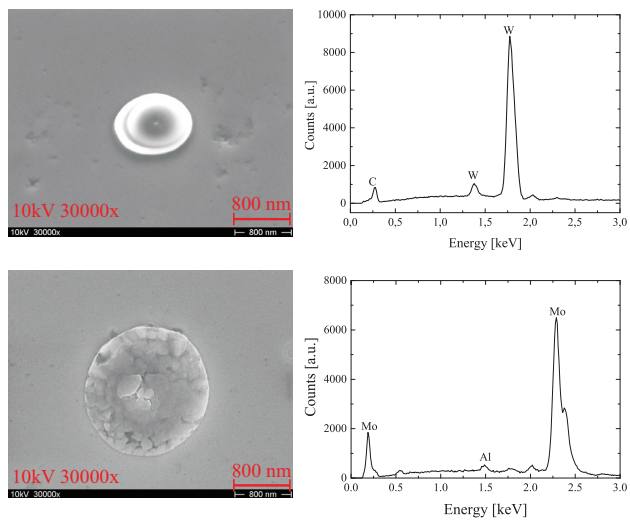

Figure 4: SEM images and EDX spectrum of an emitter with E_{on} =60 MV/m (top) and E_{on} =70 MV/m (bottom).

It is commonly known that formation of the oxides on the surface can significantly affect FE properties and particularly suppress FE [5]. To investigate the influence of HT on molybdenum oxides we used XPS, which is very sensitive to the chemical state of the surface. The shape of Mo 3d

ISBN: 978-3-95450-132-8 doi:10.18429/JACoW-IPAC2014-THPRO042

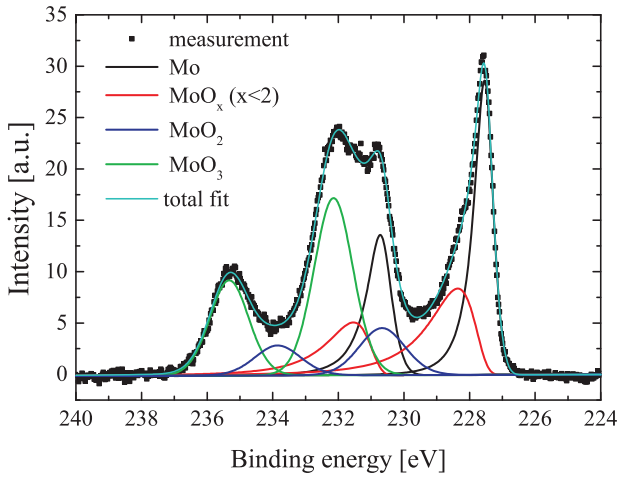

Figure 5: Mo 3d photoemission spectrum prior to the HT with deconvolution and corresponding fit curves.

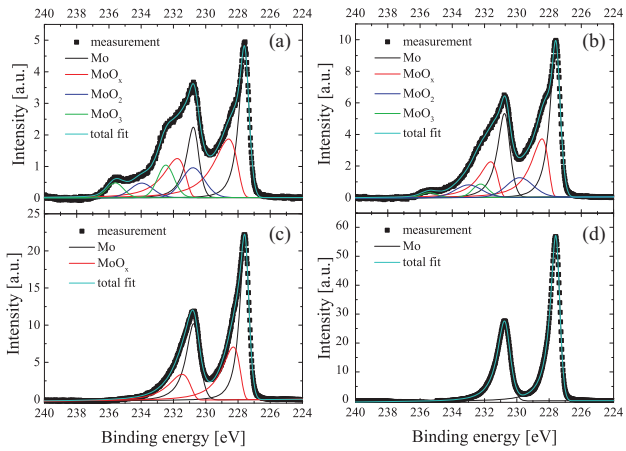

Figure 6: Mo 3d photoemission spectra after HT at 100 °C (a), 300 °C (b), 400 °C (c), and 600 °C (d).

spectrum prior to HT reveals besides metallic molybdenum the presence of conducting MoO_2, semiconducting MoO_3 (energy gap of 3 eV and a work function of 6.9 eV [6]) and nonstoichometric MoO_x oxides (Fig. 5). After deconvolution of the spectrum the weight of each component f is obtained as a ratio of the area under the corresponding peak to the total area of the spectrum. After the XPS measurement the sample was moved into a preparation chamber for a HT. Four treatment cycles were performed *in situ* with increasing temperature of 100 °C, 300 °C, 400 °C and 600 °C for 1 h, after each treatment step the sample was transferred back into the analysing chamber for the XPS measurement. The position of the illuminated area remains unchanged. The weight f for MoO_3 reduces from ~0.33 for an unnealed sample to 0.05 after HT at 300 °C (Table 1). After HT at 400 °C the molybdenum trioxide layer was removed completely (Fig. 6). After the last HT at 600 °C all Mo oxide correlated peaks disappeared, indicating that the oxide film was removed completely.

The thickness of the oxide layer can be estimated as:

$$h = -\lambda \cdot \ln\left(I/I_0\right), \qquad (2)$$

where λ is the electron inelastic mean free path (IMFP) in the oxide layer, I and I_0 are the intensities of metallic component in the XPS spectra with and without oxide layer, respectively. For MoO_3 and an electron energy of 420 eV IMFP ~ 1.1 nm, and for other oxides IMFP is nearly the same [7]. Therefore, the total oxide layer thickness prior to HT can be estimated as $h \sim 3.5$ nm (Table 1).

Table 1: Estimated Weights of Individual Oxides and Thickness of the Total Molybdenum Oxide Layer

Treatment	f (MoO_2)	f (MoO_3)	h
as received	0.11	0.33	3.5 nm
100 °C	0.14	0.11	2.7 nm
300 °C	0.14	0.05	1.9 nm
400 °C	0	0	1.1 nm

CONCLUSIONS

Preparation of bi-alkali antimonide photocathodes requires an oxide-free substrate surface. An unannealed molybdenum substrate shows no FE up to a field strength of 50 MV/m. Nevertheless, HT of the surface at 400 °C (for instance, the entire surface in the preparation chamber or local heating in the gun cavity during the current processing) switches on new emission sites and reduces E_{on} to about 20 MV/m, which is relevant for SRF cavities. Analysis of the XPS spectra showed considerable reduction of the oxide layer (inter alia MoO_3) at this temperature. We assume that molybdenum trioxide acts as a protection layer, which prevents unwanted FE. Selective removal of the oxide layer for example by irradiation with the excimer laser solely in the cathode region prior to the alkali deposition might reduce FE from the remaining substrate material.

ACKNOWLEDGMENT

This work was supported by German Bundesministerium für Bildung und Forschung project 05K13PX2, Land Berlin and grants of Helmholtz Association.

REFERENCES

[1] J. Smedley *et al.,* Proc. of FEL'13, TUPSO76, p. 403.

[2] D. Lysenkov and G. Müller, Int. J. Nanotechnol. 2 (2005) 239.

[3] R. G. Forbes, JVST B 17 (1999) 534.

[4] D. V. Vyalikh *et al.,* Synchrotron Radiat. News 15 (3) (2002) 26.

[5] A. Navitski *et al.,* Phys. Rev. ST Accel. Beams 16 (2013) 112001.

[6] M. Kröger *et al.,* Appl. Phys. Lett. 95 (2009) 123301.

[7] http://www.nist.gov/srd/nist71.cfm

Content from this work may be used under the terms of the CC BY 3.0 licence (© 2014). Any distribution of this work must maintain attribution to the author(s), title of the work, publisher, and DOI.